Article https://www.korseaj.org

Improving Transitional-Season Microclimate Control in Greenhouses Using a Dual Thermal-Storage Air-Source Heat Pump System

Seong-heon Kim [1], Sung-wook Yoon [1], Tae-seok Lee [2], Hyung-kwon Kim [3] and Jin-kyung Kwon [1*]

[1]Division of Smart Farm Development, National Institute of Agricultural Sciences, Jeonju 54875, Korea, [2]Smart Agriculture Team, Rural Development Administration, Jeonju 54875, Korea, [3]Protected Horticulture Research Institute, National Institute of Horticulture and Herbal Science, Haman 52054, Korea
* Corresponding Author: cen55@korea.kr

Abstract: Seasonal transitions in greenhouse production often cause rapid fluctuations in temperature and humidity, increasing condensation risk and stressing crop growth. This study evaluates a dual thermal-storage Air-Source Heat Pump (ASHP) system designed to stabilize the greenhouse microclimate under such variable conditions. Monthly heating and cooling loads of a semi-closed greenhouse were first estimated using EnergyPlus to determine operational requirements for thermal storage. The system incorporates a 150-ton main tank and a 60-ton auxiliary tank, enabling independent heating and cooling operation and rapid switching between modes. Field evaluation during the autumn transitional period (October~November 2025) demonstrated substantial improvements in environmental stability. The system maintained daytime cooling at 17~18℃ and nighttime heating at 18~20℃, reducing diurnal temperature fluctuation by 40% and relative-humidity variation by 30%. High-humidity durations above 85%—a critical threshold for condensation and disease development—were reduced by 35%. These outcomes indicate that the dual-storage configuration effectively buffers short-term outdoor variability, enhances dehumidification without ventilation losses, and maintains a more consistent canopy-level microclimate. Overall, the dual thermal-storage ASHP system offers a practical and energy-efficient approach for improving greenhouse climate control during transitional seasons and supporting stable crop production. Future work will focus on frost management and AI-based integrated control.

Keywords: Building energy simulation, Heat pump, Microclimate, Semi-closed greenhouse, Tomato cultivation

https://doi.org/10.5338/KJEA.2025.44.46

Agric. Environ. Sci. 2025, 44, 490-501

Received: November 17, 2025
Revised: November 25, 2025
Accepted: December 2, 2025
Published: December 8, 2025

Online ISSN: 2233-4173
Print ISSN: 1225-3537

Check for updates

Introduction

Protected horticulture is a highly energy-dependent sector as it must maintain stable crop growth conditions regardless of outdoor climate fluctuations. In recent years, the demand for precise heating and cooling control in greenhouses has increased significantly due to severe temperature variations and the growing frequency of extreme weather events induced by climate change [1,2]. According to the Rural Development Administration (RDA) and the Korea Meteorological Administration (KMA), the annual number of heatwave days in South Korea rose by about 49.5%, from an average of 91.8 days (2002~2012) to 137.7 days (2013~2022). In 2022, of the 105.4 ha of farmland damaged by cold waves, 66.8 ha (approximately 63%) were greenhouse facilities. These extreme temperature fluctuations not only challenge environmental stability but also increase plant stress and yield losses, underscoring the growing importance of reliable heating and cooling systems as essential infrastructure for sustainable greenhouse management [3].

Efforts to improve energy efficiency in greenhouse climate control have primarily focused on Ground-Source Heat Pumps (GSHPs) and Air-Source Heat Pumps (ASHPs). Both systems offer higher energy efficiency and lower greenhouse gas emissions compared with conventional oil or gas heating, but their performance and cost-effectiveness depend on heat source characteristics and ambient conditions. GSHPs provide a stable heat source largely unaffected by outdoor temperature changes [3]. Anifantis et al. [4] showed that coupling a geothermal heat pump with a solar collector achieved a stable COP (Coefficient of Performance) of 4.0~5.0, significantly reducing fuel costs and CO_2 emissions. Harjunowibowo et al. [5] reported a seasonal COP range of 1.48~2.97, emphasizing borehole depth and groundwater flow as key design factors. Conversely, ASHPs have gained rapid adoption in agriculture due to their simple structure, lower installation cost, and easy maintenance. Lim et al. [6] demonstrated that an air-to-water heat pump using underground air reduced heating costs by 70%, though its COP fell to 2.1~2.7 below 0°C. van Beveren et al. [7] showed that semi-closed greenhouses using ASHP-based cooling-dehumidification improved CO_2 retention and uniform crop growth. These studies highlight ASHP advantages but also limitations such as outdoor temperature dependency, defrost inefficiency, and difficulty in responding to mixed heating–cooling loads during transitional seasons.

A persistent issue in ASHP-based greenhouse HVAC systems is the low annual utilization rate relative to high installation costs. According to MAFRA, South Korea, ASHP installation averages about 800 million KRW per hectare (approximately 0.9 million KRW/kW), yet operation is typically limited to winter heating and summer cooling [8]. During transitional seasons, systems often stop operating as outdoor temperatures fall near optimal crop growth ranges, resulting in only 30~40% annual use. However, in these periods, greenhouses face simultaneous daytime overheating and nighttime cooling, requiring both cooling and heating. Conventional single-tank ASHP systems are inefficient under such conditions due to several-hour mode-switching delays, leading to energy loss and unstable thermal control. Therefore, this study aims to enhance year-round utilization and transitional-season performance of ASHPs by developing a dual thermal-storage air-source heat pump system. The system integrates two separate storage tanks with coordinated control to enable rapid mode switching, improve thermal efficiency, and provide stable energy management across seasonal load variations.

Results and Discussion

Analysis of monthly heating and cooling load characteristics

Simulation results indicated that the maximum heating load of the experimental greenhouse occurred in January, reaching 290.8 kW (82.7 RT), while the maximum cooling load occurred in May, reaching 408.4 kW (116.2 RT) (Fig. 1). The thermal-load pattern showed a clear seasonal bifurcation: heating demands were concentrated from November to March, whereas cooling demands dominated from May to September. Although the highest outdoor temperatures occurred in July, the cooling load temporarily decreased due to reduced solar radiation during the monsoon season, when increased cloud cover limited solar gain. A modest daytime cooling load also appeared during the cold season, while minor nighttime heating loads were observed in summer. These phenomena are attributed to excessive winter solar radiation causing daytime overheating and to nocturnal radiative cooling and ground heat loss in summer leading to temperature drops inside the greenhouse. A full validation of the BES model was not conducted in this study, as the purpose of the simulation was to analyze heating/cooling load patterns rather than to predict temperature variations.

Particularly in transitional months (March~April and October~November), alternating patterns of daytime cooling and nighttime heating were observed under outdoor diurnal temperature differences exceeding 15°C. This indicates that conventional single-mode heat pump systems have difficulty responding rapidly to alternating heating and cooling demands under large daily

https://doi.org/10.5338/KJEA.2025.44.46
Agric. Environ. Sci. 2025, 44, 490-501

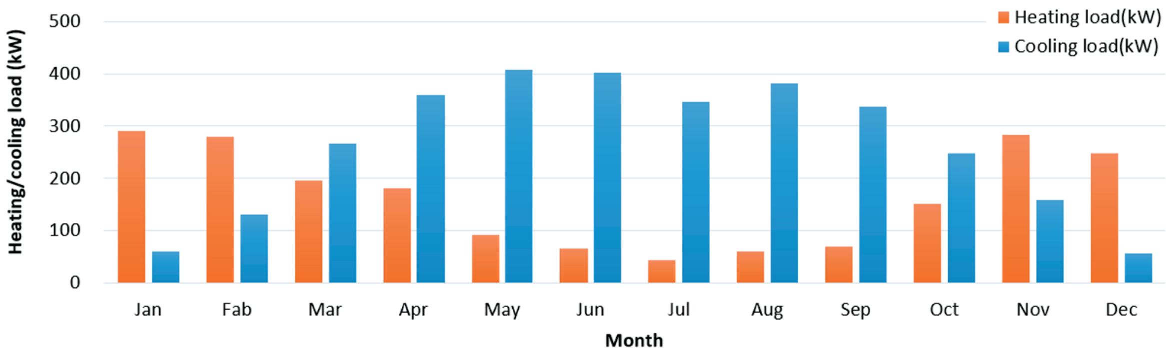

Fig. 1. Simulated monthly heating and cooling load distribution of the test greenhouse.

temperature fluctuations. These results imply that thermal loads in medium- and large-scale Korean greenhouses are governed not only by seasonal variation but also by daily temperature amplitude and solar radiation variability. In winter, rapid drops in outdoor temperature reduce the coefficient of performance (COP) of air-source heat pumps, increasing energy consumption. A daytime heat-charging and nighttime heat-discharging strategy can therefore help distribute thermal load and mitigate peak demand. Conversely, in summer, when cooling loads occur primarily in real time, it is more appropriate to reduce storage capacity and apply partial-load operation combined with peak-shaving control. Considering the maximum heating and cooling loads together with a safety factor, the total design capacity of the air-source heat pump system was set to 120 RT.

These heating–cooling patterns are consistent with earlier studies that identified solar radiation variability and large diurnal temperature swings as major drivers of short-term load fluctuations in protected horticulture. Rasheed et al. [9] reported that greenhouse thermal loads are often governed not only by seasonal trends but also by rapid intraday variations caused by solar gain and outdoor temperature changes. Similarly, Akpenpuun et al. [10] emphasized that monthly and seasonal load distributions are strongly influenced by day–night temperature amplitudes and transient weather conditions. The presence of daytime overheating in winter and nighttime temperature drops in summer observed in our simulation corresponds well to these findings and highlights the importance of designing heat pump systems capable of responding to mixed heating–cooling loads on a short-timescale basis.

Optimization of thermal storage capacity and storage temperature

Based on the simulated heating and cooling loads, the capacities of the thermal storage tanks were optimized to ensure stable operation and efficient thermal management. Fig. 2 shows the variation in storage temperature of the main thermal tank under different capacities during the heating (January~February) and cooling (July~August) seasons. When the main tank capacity exceeded 115 tons during the heating season, the storage temperature remained below 50°C, and during the cooling season, capacities up to 150 tons maintained the chilled-water temperature above 5°C. Considering both thermal stability and operational flexibility, the main thermal storage capacity was therefore set to 150 tons. The auxiliary thermal storage tank was designed to enable separate storage of chilled and heated water during transitional periods when both heating and cooling loads occur. As shown in Fig. 3, during heating operation in transitional months (March~April and October~November), an auxiliary tank capacity of 60 tons or more kept the storage temperature below 50°C, while during cooling operation, capacities of 50 tons or more maintained the chilled-water temperature above 5°C. To reliably accommodate both heating and cooling demands during these periods, the auxiliary thermal storage capacity was set to 60 tons.

Using the optimized capacities of the 150-ton main tank and 60-ton auxiliary tank, a seasonally adaptive operating strategy was established (Table 1). From December to February (heating-dominant period), the main tank operated exclusively in heating mode, with the auxiliary tank connected in parallel when necessary to distribute peak loads and reduce compressor cycling. From May to September (cooling-dominant period), the main tank was used for chilled-water production, while the auxiliary tank functioned as a supplementary cooling reservoir for peak-load relief. During transitional seasons (March~April and October~November),

https://doi.org/10.5338/KJEA.2025.44.46
Agric. Environ. Sci. 2025, 44, 490-501

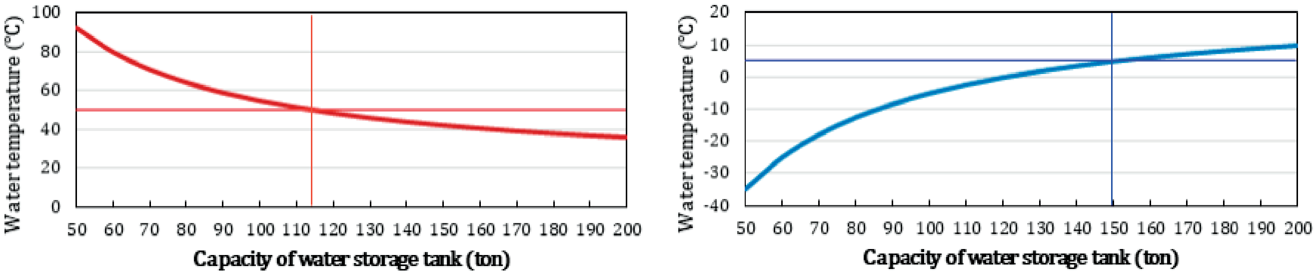

Fig. 2. Variation of storage temperature according to main tank capacity during heating and cooling seasons.

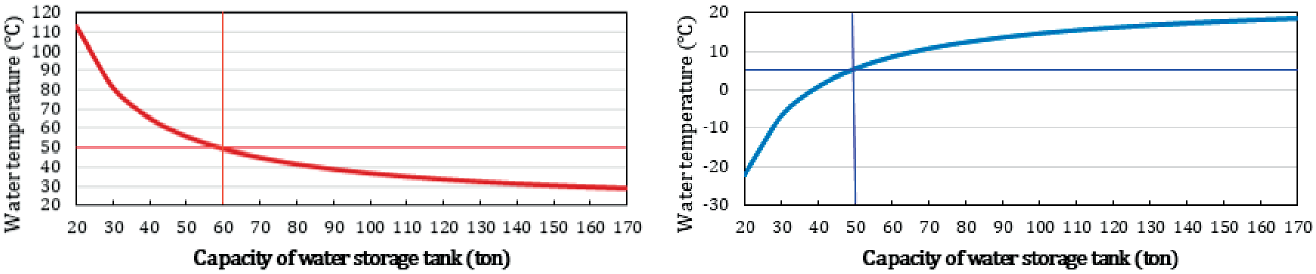

Fig. 3. Variation of storage temperature according to auxiliary tank capacity during transitional season.

Table 1. Monthly operation strategy of the dual-tank air-source heat pump system

Seasons	Months	Modes and temperatures	
		150t-tank	60t-tank
Winter	January	Heating (42.0°C)	Auxiliary heating
	February	Heating (37.1°C)	Auxiliary heating
Transition	March	Heating (30.7°C)	Cooling (13.1°C)
	April	Cooling (12.2°C)	Heating (37.4°C)
Summer	May	Cooling (8.3°C)	Auxiliary cooling
	June	Cooling (5.1°°C)	Auxiliary cooling
	July	Cooling (5.2°C)	Auxiliary cooling
	August	Cooling (6.2°C)	Auxiliary cooling
	September	Cooling (11.2°C)	Auxiliary cooling
Transition	October	Cooling (15.9°C)	Heating (24.2°C)
	November	Heating (42.4°C)	Cooling (17.5°C)
Winter	December	Heating (38.3°C)	Auxiliary heating

the main and auxiliary tanks were operated independently, enabling rapid switching between daytime cooling and nighttime heating. In March and October, when heating demand exceeded cooling demand, the main tank stored hot water and the auxiliary tank stored chilled water; in April and November, this configuration was reversed. This strategy mitigates load imbalances caused by outdoor temperature fluctuations, minimizes response delays during mode transitions, and maximizes utilization efficiency of stored thermal energy.

The selected capacities of 150 tons for the main tank and 60 tons for the auxiliary tank align with conclusions from previous work underscoring the importance of thermal buffering in heat pump systems. Anifantis et al. [11] demonstrated that stable storage temperatures significantly enhance heat pump efficiency, maintaining COP levels in the range of 4.0~5.0 when sufficient thermal mass is available. Harjunowibowo et al. [5] similarly reported that undersized storage volumes lead to excessive compressor cycling

https://doi.org/10.5338/KJEA.2025.44.46
Agric. Environ. Sci. 2025, 44, 490-501

and substantial seasonal COP degradation. The stable maintenance of charging temperatures below 50°C for heating and above 5°C for cooling in our study supports these earlier findings and suggests that the adopted dual-tank configuration provides adequate thermal inertia to accommodate both peak loads and transitional-season demands.

Construction of the dual thermal storage air-source heat pump system

Heating and cooling loads were calculated using an EnergyPlus-based building energy simulation, which indicated a maximum annual thermal load, including transitional-season demand, of approximately 120 RT. Accordingly, the total heat pump capacity was set to 120 RT, with storage capacities of 150 tons and 60 tons for the main and auxiliary tanks, respectively, reflecting the load characteristics and operating strategy. The 150-ton main tank serves as the primary reservoir for both heating and cooling throughout the year, whereas the 60-ton auxiliary tank is used mainly during transitional periods to store chilled and heated water separately. To enhance flexibility in mode switching and facilitate maintenance, three 40-RT ASHP units were installed: two connected to the main tank and one to the auxiliary tank. A valve-controlled switching mechanism allows the unit normally connected to the auxiliary tank to be reconfigured to the main tank when load concentration occurs under extreme hot or cold conditions. This enables all three units to operate in parallel on the main tank when necessary, while still preserving the auxiliary tank's storage function.

The installed system at the Department of Agricultural Engineering, National Institute of Agricultural Sciences, is shown in Fig. 4. Both tanks (150 t and 60 t) are fabricated from double-layer insulated steel panels to reduce heat loss, and the outdoor ASHP units are aligned north-south to minimize solar-radiation exposure and exhaust-air recirculation. Cross-connected piping between the tanks allows flow distribution to be adjusted according to heating and cooling demand. The principal advantage of this dual-storage configuration is the elimination of thermodynamic inefficiencies during mode transition. In conventional single-tank systems, alternating storage of chilled and hot water in the same tank induces thermal short-circuiting and 1~2 days of performance degradation during mode switching. In contrast, the dual-tank system operates heating and cooling tanks independently, preventing cross-temperature interference and substantially reducing transition time. This enhances adaptability to transitional-season load fluctuations, expands year-round utilization of ASHPs, and improves operational responsiveness and system efficiency in controlled-environment agriculture.

Fig. 4. Installed dual-tank air-source heat pump system at the test greenhouse.

https://doi.org/10.5338/KJEA.2025.44.46
Agric. Environ. Sci. 2025, 44, 490-501

The architectural features of the dual-tank design are consistent with operational characteristics highlighted in studies on semi-closed and mechanically conditioned greenhouses. van Beveren et al. [7] showed that ASHP-based cooling–dehumidification systems substantially improve CO_2 retention, microclimate uniformity, and energy-use efficiency when rapid switching between modes is possible. The separation of hot- and cold-water storage in our system addresses the thermal short-circuiting limitations commonly observed in conventional single-tank configurations. Moreover, Trépanier et al. [2] stressed that future climate conditions —characterized by more frequent extreme heat events and higher humidity—will require environmental-control systems with fast, flexible responses to shifting thermal loads. The dual-storage arrangement implemented here is well aligned with these forward-looking operational requirements.

Evaluation of heating-cooling transition and environmental stabilization

To evaluate heating-cooling transition performance and microclimate stabilization, on-site experiments were conducted from October to November 2025. Temperature and humidity in the cultivation room before and after system implementation were compared. Before installation (Fig. 5), the diurnal outdoor temperature range was about 15°C (daytime 25~26°C; nighttime 6~10°C). Nighttime heating using stored heat was achieved, but delays in switching to cooling mode during the day caused repeated indoor temperature rises above 25°C. The temperature difference between the HVAC chamber and duct outlet reached up to 3°C, indicating a sluggish response to outdoor changes and low control stability. Relative humidity (RH) dropped below 40% during daytime overheating and increased to nearly 90% at night, resulting in prolonged condensation-prone conditions. Absolute humidity remained between 0.08 and 0.15 kg/m^3, confirming limited dehumidification capability and substantial environmental fluctuations under single-tank operation. After implementation of the dual-tank ASHP system (Fig. 6), indoor temperature variability was markedly reduced under similar outdoor conditions (daytime 20~26°C; nighttime 6~10°C). Daytime Fan-Coil Unit (FCU) cooling using chilled water supplied air at 17~18°C, effectively suppressing solar-induced overheating, while nighttime heating with stored hot water maintained greenhouse temperatures at 18~20°C. As a result, the day-night temperature fluctuation decreased from ±6~8°C before installation to ±3~4°C after installation, a reduction of approximately 40%. The RH variation range similarly decreased from 40~90% to 50~85%, corresponding to a reduction of about 30% in fluctuation amplitude. The duration of RH above

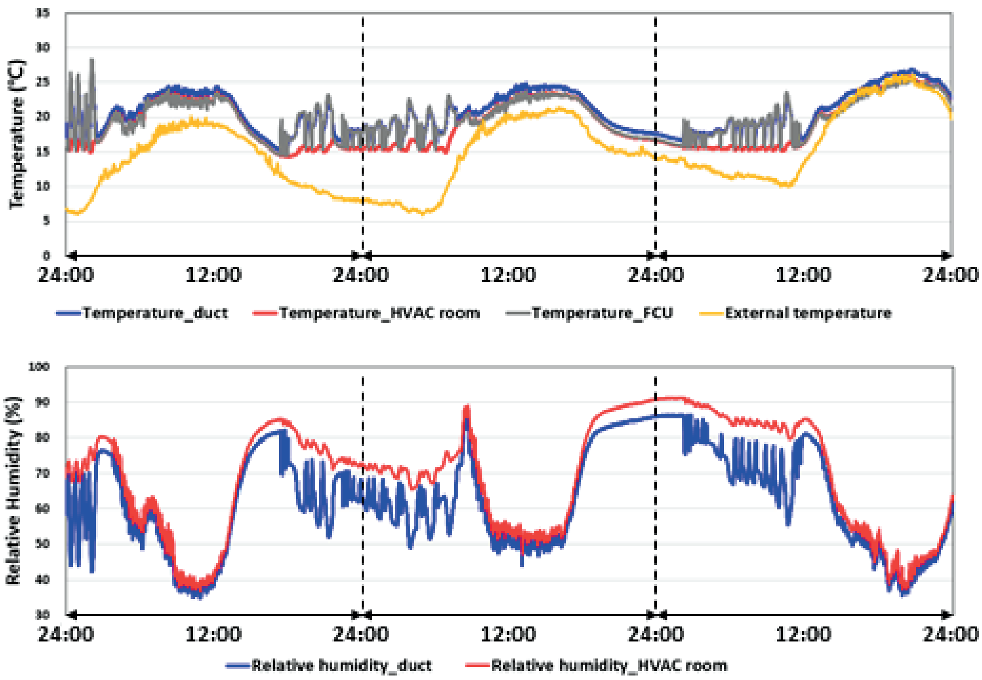

Fig. 5. Temperature and humidity responses in the cultivation room before system application.

https://doi.org/10.5338/KJEA.2025.44.46
Agric. Environ. Sci. 2025, 44, 490-501

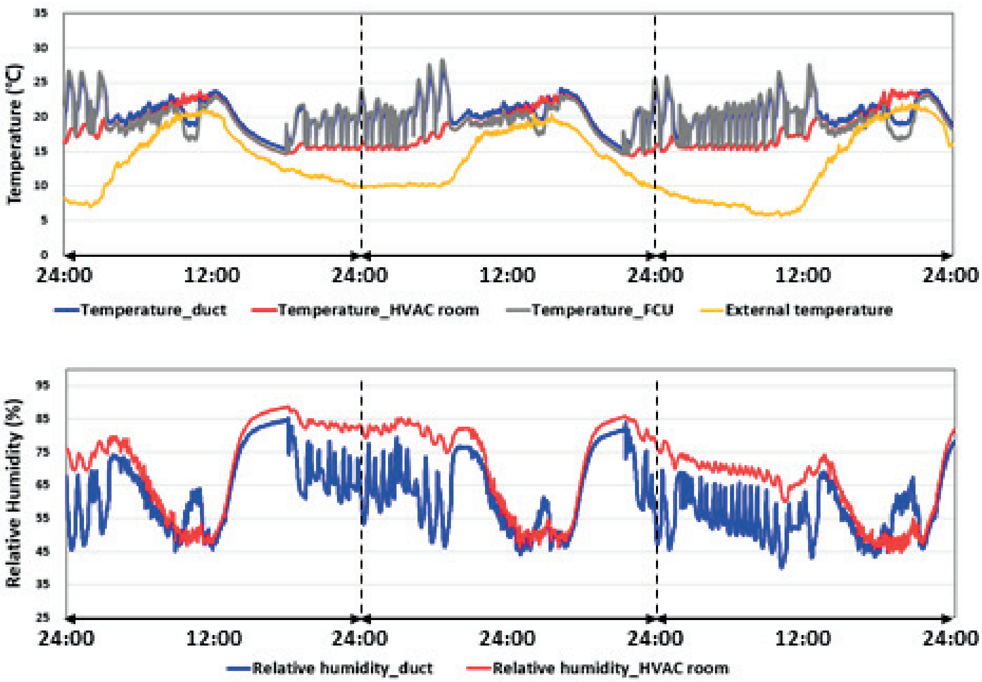

Fig. 6. Temperature and humidity responses in the cultivation room after system application.

85%, associated with condensation risk, was reduced by approximately 35%, indicating a lower potential for pathogen development and crop disease. Absolute humidity stabilized at 0.09~0.13 kg/m^3, and the difference between greenhouse air and HVAC chamber air almost disappeared, suggesting improved heat and moisture exchange efficiency of the conditioned air.

The observed reductions in temperature variability (40%) and RH fluctuation (30%) are in good agreement with previous findings regarding the benefits of rapid cooling and dehumidification in greenhouse climate management. Lee et al. [8] reported that delays in cooling initiation can intensify daytime overheating and accelerate nighttime RH accumulation, ultimately increasing physiological stress and disease susceptibility. Fanourakis et al. [1] further emphasized that prolonged RH above 85% significantly heightens condensation risks and promotes fungal pathogen development. The roughly 35% reduction in high-humidity duration in our study therefore represents a meaningful improvement in disease-risk mitigation. The stabilization of absolute humidity between 0.09 and 0.13 kg/m^3 also corresponds to the dehumidification performance reported by van Beveren et al. [7], who found that ASHP-based latent cooling can effectively remove moisture without relying on ventilation, avoiding both CO_2 losses and thermal disturbances. Additionally, the system's rapid heating–cooling switching ability directly addresses the climate-change-related operational challenges highlighted by Trépanier et al. [2], who predicted increasing cooling demands and sharper nighttime temperature declines in protected horticulture. Collectively, these results affirm that the dual thermal-storage configuration provides a robust and responsive strategy for improving microclimate stability during transitional seasons.

These results demonstrate that the dual thermal-storage configuration facilitates rapid switching between heating and cooling modes and buffers rapid outdoor fluctuations through energy exchange between the two tanks. In particular, during transitional-season daytime cooling and dehumidification, the system maintained stable air temperature while suppressing condensation risk. Overall, the dual-tank ASHP system and associated seasonal operating strategy reduced day-night temperature variation by about 40%, RH fluctuations by 30%, and condensation-risk duration by 35%. This improvement in thermal stability and microclimatic uniformity provides a practical foundation for energy-efficient and quality-oriented greenhouse climate control, especially during transitional periods.

https://doi.org/10.5338/KJEA.2025.44.46
Agric. Environ. Sci. 2025, 44, 490-501

Conclusion

This study developed and validated a dual thermal-storage system designed to improve microclimate stability and operational flexibility in greenhouse crop production. Using Building Energy Simulation (BES), monthly heating and cooling loads were quantified, allowing the selection of a 150-ton main tank and a 60-ton auxiliary tank as an optimal thermal-storage configuration capable of responding to strong seasonal and diurnal fluctuations. By separating heating and cooling storage, the dual-tank design eliminated the mode-transition delays and thermal short-circuiting typically observed in conventional single-tank systems. Field verification during the transitional season (October~November 2025) demonstrated clear improvements in the greenhouse environment. The system maintained daytime cooling temperatures of 17~18°C and nighttime heating temperatures of 18~20°C, while stabilizing relative humidity around the crop-optimal range. As a result, daily temperature fluctuations decreased by over 40%, RH variation decreased by roughly 30%, and the duration of condensation-risk conditions was reduced by 35%. This enhancement in thermal and humidity stability is expected to lower pathogen pressure, reduce physiological stress, and improve the uniformity of the crop-growing environment. Additionally, internal circulation-based dehumidification was achieved without ventilation losses, suggesting potential benefits for both crop quality and energy conservation.

Overall, the findings indicate that dual thermal-storage ASHP systems can serve as a practical and scalable year-round environmental control solution for protected horticulture, especially during periods characterized by rapidly shifting heating and cooling demands. Future work should evaluate crop-level responses, assess long-term impacts on disease incidence and yield stability, and integrate AI-driven control strategies to further optimize heating, cooling, and dehumidification. With such advancements, ASHP technology may play a central role in sustainable and climate-responsive greenhouse management systems.

Materials and Methods

Estimation of heating and cooling loads using building energy simulation

Building Energy Simulation (BES) was used to estimate monthly heating/cooling loads and provide design inputs for the thermal-storage heat pump system. BES predicts building energy consumption through three steps: model preparation, simulation execution, and result analysis. Key inputs included building geometry, material thermal properties, HVAC specifications, operating schedules, internal heat gains, and TMY climate data [9-12]. During the modeling stage, the geometric configuration of the building, thermal properties of construction materials, HVAC system specifications and efficiencies, operational schedules, internal heat gains, and the site-specific Typical Meteorological Year (TMY) climate data were defined. In the simulation execution stage, the selected BES code compiled the model and computed the dynamic heating and cooling loads on an hourly or daily basis. The analysis stage subsequently produced outputs such as heating and cooling energy consumption, time of peak load occurrence, contributing factors, and potential energy-saving scenarios.

EnergyPlus (U.S. DOE), an integrated simulation engine supporting detailed thermal analysis and weather-data processing [13], was used to calculate monthly peak loads. These outputs served as the basis for determining heat pump capacity and thermal-storage requirements.

Experimental greenhouse and 3D model development

The development and validation of the dual thermal-storage Air-Source Heat Pump (ASHP) system were conducted using the experimental greenhouse located on the premises of the Department of Agricultural Engineering, National Institute of Agricultural Sciences, Rural Development Administration, South Korea (35.82624, 127.06038). The greenhouse adopts a semi-closed structure, designed to minimize direct natural ventilation and to control heating, cooling, dehumidification, CO_2 concentration,

https://doi.org/10.5338/KJEA.2025.44.46
Agric. Environ. Sci. 2025, 44, 490-501

and air circulation through a fully mechanical environmental-control system. This configuration minimizes the influence of outdoor climatic conditions, thereby improving the thermal stability of the internal environment and enhancing the reproducibility of simulation results.

For the Building Energy Simulation (BES), a three-dimensional (3D) model of the greenhouse was created from existing two-dimensional architectural drawings using the architectural Computer-Aided Design (CAD) software SketchUp. The model included detailed representations of the main structural and functional components, such as the steel frame, cultivation zones, air-handling room, corridors, offices, storage spaces, and covering materials. To accurately reproduce solar trajectory and shading effects, the actual site orientation was applied, with an azimuth angle of +13.5° eastward from true south. This adjustment enabled precise simulation of solar altitude, direct and diffuse radiation, and the resulting solar heat-gain distribution, thereby improving the accuracy of the predicted solar gains and thermal-load estimates (Fig. 7). The completed 3D geometry was then converted into an EnergyPlus input data file (IDF) and imported into the simulation environment. Through this model, the monthly and annual heating and cooling energy loads of the experimental greenhouse were calculated.

Boundary conditions and material properties

Boundary conditions define the physical parameters-such as temperature, heat flux, convective coefficients, and radiative properties-at the outer surfaces of the simulation domain (e.g., outdoor air, indoor space, and ground). They are essential to ensuring the accuracy and physical realism of simulation outcomes. The surface states and thermal properties of the greenhouse components were defined and applied in the simulation. Since both the roof and wall were covered with the same polyethylene (PE) film material, identical thermal properties were assigned to these surfaces. The ground surface was modeled using a standard ground heat transfer model to account for heat conduction with the subsurface soil, and the foundation's thermal resistance and surface emissivity were also considered. The primary thermophysical parameters used in the simulation included density, specific heat capacity, thermal conductivity, emissivity, and transmittance. These properties were obtained from the default EnergyPlus material

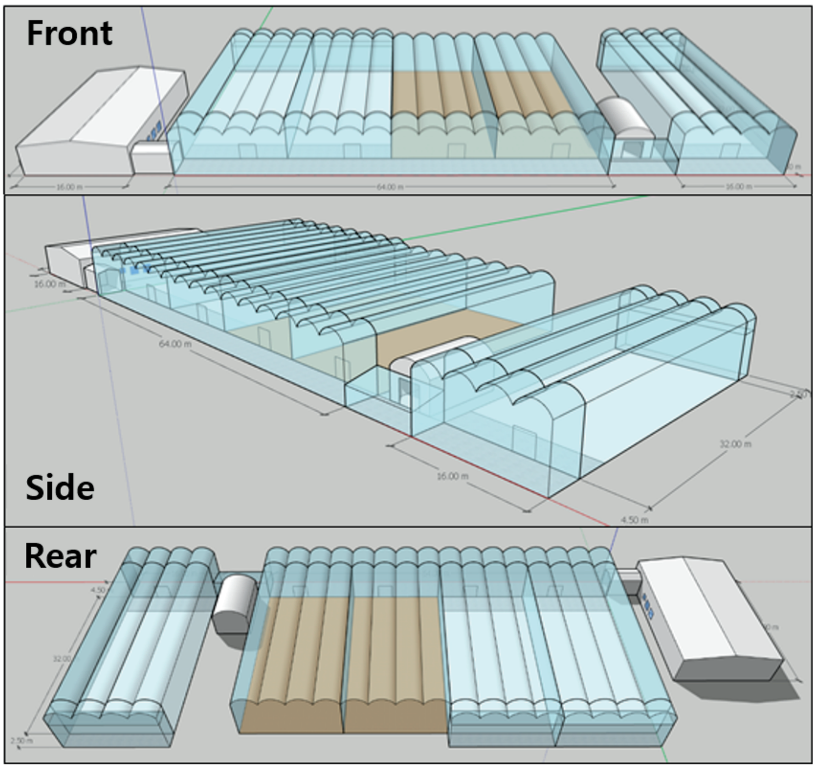

Fig. 7. Three-dimensional model of the semi-closed test greenhouse for simulation.

https://doi.org/10.5338/KJEA.2025.44.46
Agric. Environ. Sci. 2025, 44, 490-501

library and cross-validated with data from previous studies on agricultural greenhouse structures [14,15].

Meteorological data and indoor target conditions

The Standard Weather Data (SWD) represent statistically processed datasets that characterize the long-term climatic conditions of a specific region. These datasets are widely used in building energy analysis, environmental simulation, and climate-impact assessments. Typically, SWD include key meteorological variables-such as air temperature, relative humidity, solar radiation, wind speed and direction, precipitation, and atmospheric pressure-observed over a period exceeding ten years, thereby representing the region's average annual climate conditions. In this study, standard weather data representative of the Jeonju region, Jeollabuk-do, where the experimental greenhouse is located, were utilized. The dataset was developed by the Korean Passive Building Association (KPBA) based on fifteen years (2007~2021) of measured meteorological observations and was provided in the EnergyPlus Weather (EPW) file format. The EPW file contains all major input parameters required for dynamic thermal simulation, including outdoor air temperature, relative humidity, direct and diffuse solar radiation, wind velocity and direction, and precipitation. The indoor temperature set-points for the simulation were determined according to the standard cultivation conditions for tomato (Lycopersicon esculentum Mill.), as defined by the National Institute of Agricultural Sciences, South Korea. Accordingly, the target temperatures were specified as 24°C during daytime and 17°C at night throughout the year to represent the optimal thermal environment for tomato production.

Design of the air-source heat pump and thermal storage system

Based on the monthly heating and cooling loads obtained from the Building Energy Simulation (BES), the required specifications of the dual thermal-storage Air-Source Heat Pump (ASHP) system were determined. The total heating capacity of the heat pump was calculated by considering the maximum annual thermal load. To determine the capacities of the two thermal-storage tanks, full-load and partial-load storage strategies were considered for cooling and heating operations, respectively. In the full-load storage mode, all thermal energy generated by the heat pump is stored in the thermal tank and later supplied to meet the load independently. In contrast, the partial-load storage mode allows the heat pump to respond directly to the load while simultaneously charging the storage tank with excess heat. For the ASHP, the COP decreases sharply in winter due to frost formation and low ambient temperatures; therefore, a daytime charging/nighttime discharging partial-load operation was applied for heating. During cooling periods, however, COP variation is relatively small, and thus full-load storage operation was adopted. The required thermal-storage capacity and optimal storage temperature were then calculated using Eq. (1):

$$M = \frac{Q_{load} \times t}{\rho c_p \Delta T} \quad \text{Eq. (1)}$$

where M is the required mass of the storage medium (kg, water), Q_{load} is the heating or cooling load (kW), t is the system operating time (h), c_p is the specific heat capacity of water (J/kg·K), and ΔT is the temperature difference between the inlet and outlet of the storage tank (°C). Here, the outlet temperature corresponds to the storage-tank set-point (charging temperature), while the inlet temperature represents the return water temperature after greenhouse heat exchange-i.e., the target heating or cooling temperature. The storage-tank capacities were determined by first simulating the temperature variation according to tank size and then selecting the heat pump capacity that maintained storage temperatures within the recommended ranges (heating ≤ 50°C, cooling ≥ 5°C). From the selected configuration, the optimal storage temperature was derived. Operating hours were determined based on field-manager experience and actual operation data. For the main storage tank, 12 h of operation was applied during extreme-cold heating and 9 h during peak-summer cooling. For the auxiliary storage tank, 9 h of heating and 3 h of cooling were assigned for transitional-season operation.

https://doi.org/10.5338/KJEA.2025.44.46
Agric. Environ. Sci. 2025, 44, 490-501

System performance evaluation

System performance was evaluated during October-November 2025. Measurements included air temperature and relative humidity in the air-handling room, FCU supply-air temperature, duct air conditions, and central-zone microclimate. Data were logged at 1-minute intervals. Missing values and outliers were corrected using IQR-based filtering and a three-point moving average. Pre- and post-installation periods were compared using hourly averages under similar outdoor conditions.

Data Availability: All data are available in the main text or in the Supplementary Information.

Author Contributions: S.-h. conducted the overall research, performed the building energy simulation, and designed the heat-pump and thermal-storage system. S.-w., T.-s., and H.-k. contributed to data curation and interpretation. J.-k. supervised the research process and served as the corresponding author.

Notes: The authors declare no conflict of interest

Acknowledgments: This work was carried out with the support of “Cooperative Research Program for Agriculture Science & Technology Development (Project No. PJ01742401)”, Rural Development Administration, Republic of Korea.

Additional Information:
Supplementary information The online version contains supplementary material available at https://doi.org/10.5338/KJEA.2025.44.46
Correspondence and requests for materials should be addressed to Jin-kyung Kwon.
Peer review information Agricultural and Environmental Sciences thanks the anonymous reviewers for their contribution to the peer review of this work.
Reprints and permissions information is available at http://www.korseaj.org

References

1. Fanourakis D, Tsaniklidis G, Makraki T, Nikoloudakis N, Bartzanas T, Sabatino L, Fatnassi H, Ntatsi G (2025) Climate change impacts on greenhouse horticulture in the mediterranean basin: Challenges and adaptation strategies. Plants, 14(21), 3390. https://doi.org/10.3390/plants14213390.
2. Trépanier MP, Gosselin L, Schwarz PO (2024) Simulating the impact of climate change on energy consumption and yield in Canadian greenhouse horticulture. Sustainable Futures, 8, 100354. https://doi.org/10.1016/j.sftr.2024.100354.
3. Ju OJ, Soh H, Lee SW, Lee YS (2022) Climate-Smart Agriculture (CSA)-based assessment of a local rice cultivation in Hwaseong-city, Gyeonggi-do. Korean Journal of Environmental Agriculture, 41(1), 32-40. https://doi.org/10.5338/KJEA.2022.41.1.05.
4. Anifantis AS, Pascuzzi S, Scarascia-Mugnozza G (2016) Geothermal source heat pump performance for a greenhouse heating system: An experimental study. Journal of Agricultural Engineering, 47(3), 164-170. https://doi.org/10.4081/jae.2016.544.
5. Harjunowibowo D, Omer SA, Riffat SB (2021) Experimental investigation of a ground-source heat pump system for greenhouse heating–cooling. International Journal of Low-Carbon Technologies, 16(4), 1529-1541. https://doi.org/10.1093/ijlct/ctab052.
6. Lim TS, Baik YK, Kim DD (2020) Heating performance analysis of an air-to-water heat pump using underground air for greenhouse farming. Energies 13(15), 3863. https://doi.org/10.3390/en13153863.
7. van Beveren PJM, Bontsema J, van Straten G, van Henten EJ (2020) Optimal utilization of energy equipment in a semi-closed greenhouse. Computers and Electronics in Agriculture, 179, 105800. https://doi.org/10.1016/j.compag.2020.105800.
8. Lee T, Kim J, Park S, Lee C (2021) Analysis of the effect of fog cooling during daytime and heat pump cooling at night on greenhouse environment and plants in summer. Journal of Bio-Environment Control, 30(4), 328-334. https://doi.org/10.12791/KSBEC.2021.30.4.328.
9. Rasheed A, Lee JW, Lee HW (2015) A review of greenhouse energy management by using building energy simulation. Journal of Bio-Environment Control, 24(4), 317-325. https://doi.org/10.12791/KSBEC.2015.24.4.317.
10. Akpenpuun TD, Ogunlowo QO, Rabiu A, Adesanya MA, Na WH, Omobowale MO, Mijinyawa Y, Lee HW (2022) Building energy simulation model application to greenhouse microclimate, covering material and thermal blanket modelling: A review. Nigerian Journal of Technological Development, 19(3), 276-286. https://doi.org/10.4314/njtd.v19i3.10.

11. Pan Y, Zhu M, Lv Y, Yang Y, Liang Y, Yin R, Yang Y, Jia X, Wang X, et al. (2023) Building energy simulation and its application for building performance optimization: A review of methods, tools, and case studies. Advances in Applied Energy, 10, 100135. https://doi.org/10.1016/j.adapen.2023.100135.
12. Yigit S, Ozorhon B (2018) A simulation-based optimization method for designing energy efficient buildings. Energy and Buildings, 173, 10-23. https://doi.org/10.1016/j.enbuild.2018.08.045.
13. Crawley DB, Lawrie LK, Winkelmann FC, Buhl WF, Huang YJ, Pedersen CO, Strand RK, Liesen RJ, Fisher DE, et al. (2001) EnergyPlus: creating a new-generation building energy simulation program. Energy and Buildings, 33(4), 319-331. https://doi.org/10.1016/S0378-7788(00)00114-6.
14. Kim HK, Lee SY, Kwon JK, Kim YH (2022) Evaluating the effect of cover materials on greenhouse microclimates and thermal performance. Agronomy 12(1), 143. https://doi.org/10.3390/agronomy12010143.
15. Kim HK, Ryou YS, Kim YH, Lee TS, Oh SS, Kim YH (2021) Estimating the thermal properties of the cover and the floor in a plastic greenhouse. Energies, 14(7), 1970. https://doi.org/10.3390/en14071970.

https://doi.org/10.5338/KJEA.2025.44.46
Agric. Environ. Sci. 2025, 44, 490-501